Multicomponent Swelling of Polymer Networks

Oluwasijibomi Okeowo[†] and John R. Dorgan*

Department of Chemical Engineering, Colorado School of Mines, Golden, Colorado 80401

Received August 9, 2006; Revised Manuscript Received September 6, 2006

ABSTRACT: A mathematical model for treating multicomponent equilibrium in polymer networks is developed and tested against experimental data. Equations and numerical solution procedures for treating the full equilibrium problem of a binary mixed solvent in contact with a cross-linked polymeric network are provided. Case studies are presented for different values of the cross-link density (ρ_e) and Flory−Huggins interaction parameters (solute-1/solute-2 (χ_{12}), solute-1/network-3 (χ_{13}), and solute-2/network-3 (χ_{23})). Novel phenomena are observed in certain cases including *decreasing* concentration in the membrane with *increasing* component concentration in the contacting mixture. A simple renormalization procedure for capturing concentration dependence of the solute−network interaction parameters is proposed. Experiments on the swelling of poly(acrylonitrile-*co*-butadiene) (NBR rubber) by benzene−cyclohexane mixtures are also presented. Data obtained include cross-link densities from modulus measurements and interaction parameters χ_{13} and χ_{23} from pure component swelling. On the basis of these pure component data, no adjustable parameters are needed to predict the equilibrium swelling for the six different films studied. Model predictions based on pure component data using the renormalization approach show better agreement than the predictions based on constant interaction parameters.

Introduction

Swelling of polymer networks is an important technical topic in a wide variety of technologies including, but not limited to, membrane science, biochemical protective clothing, and hydrogels for the controlled release of drugs and other agents. Despite this technological importance, relatively little theoretical attention has been placed on understanding multicomponent effects in cross-linked polymers.

In membrane separations of binary liquid mixtures, solubility data are used to characterize the suitability of the membrane for the intended separation; typically, dense polymeric films are immersed in pure components and their mixtures to obtain solubility data. For example, Park et al. studied the sorption of alcohol−toluene mixtures in poly(acrylic acid)−poly(vinyl alcohol) blends,[1] Wang and co-workers have investigated hexane, cyclohexane, and benzene in segmented poly(ethylene oxide imide)s,[2] and Meuleman has studied mixtures of toluene and water in EPDM membranes.[3] Of these, only the study of Meuleman presents a bona fide mathematical treatment of ternary phase equilibria using experimental values for the activity of toluene in water.

Swollen networks also find significant use as hydrogels for biological applications.[4] For example, so-called "smart hydrogels" useful for bioseparations have been discussed by Kim and Park[5] and Wang and co-workers.[6] McKenna and Horkey studied poly(vinyl alcohol) hydrogels to determine the dependence of the water−matrix interaction parameter on cross-link density. For such binary systems, a linear dependence of the interaction parameter as a function of cross-link density was previously established by McKenna et al. for nonaqueous systems.[7]

The theoretical understanding of swelling has a long history. The seminal work in the field was completed by Flory and Rehner in 1943.[8] Since then, a large number of researchers have applied this theory to various cases to describe the sorption equilibrium of cross-linked polymers exposed to single solute. On the basis of these results, the interaction parameter is found to be concentration,[9,10] temperature,[10,11] and also cross-link density dependent.[7,11,12] In other swelling studies, the specific form of the rubber elasticity term in the free energy has also been the subject of several studies.[10,13−15] Also, considerable efforts have been put into understanding swelling in electrolytes and hydrogen bonding solvents.[16,17] From a more fundamental perspective, it has been recognized that the separation of the elastic and mixing free energies is not justified, and a more comprehensive theory must start with a fundamentally different partition function.[13,18]

The extension of the Flory−Rehner theory to ternary systems was considered as early as the mid-1950s by Krigbaum and Carpenter.[19] These researchers developed approximate solutions in terms of the ratios of component concentrations present in the network phase. The first experimental study aimed at testing these expressions appears to be that of Bristow.[20] Experimental and theoretical predictions were reported to be in reasonable accord for nonpolar mixtures but less satisfactory for mixtures of nonpolar and polar solutes; the lack of knowledge on the solute−solute interaction parameter was suggested to be responsible for the latter.[20] Developments in treating the thermodynamics of the ternary system consisting of two solutes in equilibrium with a swollen polymer network are most prevalent in the literature on permselective membranes; these developments include the introduction of an empirical correction term to capture concentration dependence of the interaction parameters[21] and the use of a nonlinear concentration-dependent form for the interaction parameters[22] based on an earlier treatment using a linear functional form in un-cross-linked ternary systems.[23] The constant χ parameter model has been applied to benzene−cyclohexane in polyisoprene system,[24] and the linear concentration dependent model has been applied to the toluene−water in ethylene−propylene rubber (EPR).[3] Iwatsubo and coworkers[25,26] calculated phase diagrams for the swelling equilibrium of an ionic polymer gel soaked in a solution of two mixtures, using a modified Flory−Huggins model. Jonquieres et al.[27] used a power law ($\chi = a\phi^b$) for the interaction parameter to account for the dependence of the Flory−Huggins interaction

* To whom correspondence should be addressed. E-mail: jdorgan@mines.edu.

[†] Present address: Chevron Energy Technology Company, 100 Chevron Way, Richmond, CA 94802.

10.1021/ma0618124 CCC: $33.50
Published on Web 10/20/2006

parameter on penetrant concentration in the case of vapor sorption of pure solutes in polyurethaneimide, a physically cross-linked material. This latter approach was based on earlier work by Koningsveld and Kleintjens[28] that uses a three-parameter law for the interaction parameter to describe the concentration dependence of the interaction parameter in multicomponent polymer solutions. Nandi and Winter in 2005[29] extended the Flory−Rehner theory to study the swelling behavior of partially cross-linked polymers. In their study, they assumed that a partially cross-linked polymer in contact with a solvent constitute a ternary system comprising of a polymer network, an unattached polymer (sol macromolecules), and solvent. By neglecting the interaction between sol macromolecules and network strands and also by assuming that the sol macromolecules and the network polymer are chemically similar, they were able to describe the ternary system using a single interaction parameter; that is, as a pseudobinary system.

It is apparent that many modifications to the multicomponent Flory−Rehner theory attempt to describe the concentration dependence of the interaction parameters. However, this use of an experimentally determined fitting parameter complicates the task of *predicting* preferential sorption.[30] In this paper a simple renormalization scheme is proposed that obviates the need for adjustable parameters.

The renormalization is based on a simple volume fraction weighted mixing rule involving solute−solute and solute−network interaction parameters. This renormalization better describes cosolvency effects observed in multicomponent systems when compared to the constant interaction parameters treatment; supporting data on the benzene−cyclohexane in poly(acylonitrilebutadiene) system are presented. Of utmost importance here is the fact that no adjustable parameters were used in the model to predict the equilibrium swelling of six network films—data on the binary systems are collected and used to predict the ternary behavior. It is demonstrated that the renormalization of the interaction parameters improves the predictive power of the theory when compared to the case when constant interaction parameters are used. In addition, several case studies are presented to elucidate the effects of cross-linking density, molar volumes, and interaction parameters on the relative solubility of the two solutes.

Theory and Calculations

The Flory−Rehner theory is extended in this paper to describe multicomponent sorption in cross-linked polymer films. The theory is constructed, in the usual way, from a total free energy per unit volume consisting of contributions due to the free energy of mixing and the free energy of elastic deformation. In the present development, expressions are provided to describe the ternary system consisting of solute-1, solute-2, and a cross-linked polymer network-3. The membrane is viewed as a homogeneous network characterized by a cross-link density and mean-field interaction parameters with each of the two solutes. The contacting binary liquid phase consisting of the two solutes is treated in a consistent fashion; the free energy of this contacting phase consists only of the usual free energy of mixing terms.

The free energy of the network is taken to be separable into terms associated with the free energy of mixing and of elastic deformation as expressed in eq 1.

$$\Delta G = \Delta G_{\mathrm{M}} + \Delta G_{\mathrm{E}} \tag{1}$$

where ΔG is the total free energy change per unit volume, ΔG_{m} is the free energy of mixing, and ΔG_{el} is the elastic free energy. For a ternary system consisting of two solutes and a polymer, the free energy of mixing can be written[31] as

$$\Delta G_{\mathrm{M}} = kT[n_1 \ln \varphi_1 + n_2 \ln \varphi_2 + n_3 \ln \varphi_3 + \chi_{12} n_1 \varphi_2 + \chi_{13} n_1 \varphi_3 + \chi_{23} n_2 \varphi_3] \tag{2}$$

where n_i is the number of molecules of component i, φ_i is the volume fraction of component i in the network, χ_{ij} is the interaction parameter between species i and j, k is Boltzmann's constant, and T is temperature. As discussed in the Introduction, different forms for the elastic free energy can be adopted; here the original Flory−Rehner form is used as expressed in eq 3.

$$\Delta G_{\mathrm{E}} = \left(\frac{kT\upsilon_e}{2}\right)(\alpha_x^{\,2} + \alpha_y^{\,2} + \alpha_z^{\,2} - 3 - \ln(\alpha_x\alpha_y\alpha_z)) \tag{3}$$

In eq 3, α_p is the deformation factor in the p-direction and ν_{e} is the effective number of chains between cross-links.

Differentiation of the free energy with respect to the component mole number provides expressions for the chemical potentials of the two solute species. These formulas are given by eqs 4 and 5.

$$\frac{\mu_1 - \mu_1^0}{RT} = \frac{\Delta\mu_{1\mathrm{m}}}{RT} = \ln \varphi_{1\mathrm{m}} + 1 - \varphi_{1\mathrm{m}} - \frac{V_1}{V_2}\varphi_{2\mathrm{m}} + \chi_{12}\varphi_{2\mathrm{m}}(1 - \varphi_{1\mathrm{m}}) + \chi_{13}\varphi_3(1 - \varphi_{1\mathrm{m}}) - \chi_{23}\frac{V_1}{V_2}\varphi_{2\mathrm{m}}\varphi_3 + \rho_{\mathrm{e}}V_1(\varphi_3^{\,1/3} - 0.5\varphi_3) \tag{4}$$

$$\frac{\mu_2 - \mu_2^0}{RT} = \frac{\Delta\mu_{2\mathrm{m}}}{RT} = \ln \varphi_{2\mathrm{m}} + 1 - \varphi_{2\mathrm{m}} - \frac{V_2}{V_1}\varphi_{1\mathrm{m}} + \chi_{12}\frac{V_2}{V_1}\varphi_{1\mathrm{m}} - \chi_{13}\frac{V_2}{V_1}\varphi_{1\mathrm{m}}\varphi_3 + \chi_{23}(\varphi_{1\mathrm{m}} + \varphi_{2\mathrm{m}})\varphi_3 + \rho_{\mathrm{e}}V_2(\varphi_3^{\,1/3} - 0.5\varphi_3) \tag{5}$$

where μ_i and μ_i^0 are the chemical potentials in the membrane and at the reference state, respectively. Also, ρ_{e} is the cross-link density (mol/cm^3), and V_i is the molar volume of component i. The subscript "m" denotes that these concentrations are in the network or membrane phase. In the derivation of eqs 4 and 5 the following assumptions are implicitly made: (i) the network is amorphous and homogeneous and it swells isotropically ($\alpha_x = \alpha_y = \alpha_z$), and (ii) because the network is a single molecule ($n_3 = 1$) whereas there are large numbers of solute molecules, n_3 is equated to zero. Equations 4 and 5 above have been presented previously by Mueleman and co-workers in the context of a model for membrane separations.[3]

Chemical potentials for components 1 and 2 in the contacting liquid phase are taken as being described by the equivalent of the above model but based only on a binary free energy of mixing. The resulting forms are given by eqs 6 and 7, respectively.

$$\frac{\Delta\mu_{1\mathrm{s}}}{RT} = \ln \varphi_{1\mathrm{s}} + 1 - \varphi_{1\mathrm{s}} - \frac{V_1}{V_2}\varphi_{2\mathrm{s}} + \chi_{12}(1 - \varphi_{1\mathrm{s}})^2 \tag{6}$$

$$\frac{\Delta\mu_{2\mathrm{s}}}{RT} = \ln(1 - \varphi_{1\mathrm{s}}) + \varphi_{2\mathrm{s}} - \frac{V_2}{V_1}\varphi_{1\mathrm{s}} + \chi_{12}\frac{V_2}{V_1}\varphi_{1\mathrm{s}}^{\,2} \tag{7}$$

The subscrip "s" in the above equations denotes compositions in mixed solvent phase.

The condition for equilibrium is equality of the chemical potentials in the two phases

$$\Delta\mu_{1m} = \Delta\mu_{1s} \tag{8}$$

$$\Delta\mu_{2m} = \Delta\mu_{2s} \tag{9}$$

By substituting the expression $\varphi_3 = 1 - \varphi_{1m} - \varphi_{2m}$ in eqs 4 and 5 and eliminating φ_{2s} by using $\varphi_{2s} = 1 - \varphi_{1s}$ in eqs 6 and 7, the phase equilibrium problem becomes well posed. Namely, eqs 8 and 9 can be solved for the two unknown solute concentrations in the membrane, $\varphi_{1m} - \varphi_{2m}$, as a function of the specified solution concentration, φ_{1s}.

The derivation of the chemical potentials above assumed constant interaction parameters; but it is known that these parameters can be concentration dependent. An underappreciated result from multiple component phase equilibria calculations involving small molecule system is that the interaction parameters are often rescaled to reflect the changing composition of the phases at equilibrium.[32] The simplest way to do this is to take a weighted average. Therefore, a renormalization of χ_{13} and χ_{23} is proposed in eqs 10 and 11 to give "effective" interaction parameters.

$$\chi_{13}^{e} = (1 - \varphi_{2m})\chi_{13} + \varphi_{2m}\chi_{12} = \chi_{13} + (\chi_{12} - \chi_{13})\varphi_{2m} = a_{13} + b_{13}\varphi_{2m} \tag{10}$$

$$\chi_{23}^{e} = (1 - \varphi_{1m})\chi_{23} + \varphi_{1m}\chi_{12} = \chi_{23} + (\chi_{12} - \chi_{23})\varphi_{1m} = a_{23} + b_{23}\varphi_{1m} \tag{11}$$

In these equations, $a_{i3} = \chi_{i3}$ (the constant solute−polymer interaction parameter determined from pure component swelling) and $b_{i3} = \chi_{12} - \chi_{i3}$, where $i = 1, 2$. The idea of the renormalization is to account for the effect of the third component on the usual binary interaction parameter; in essence, the mean field of interaction between two components is modified depending on the overall composition. Consider the limits bounding φ_{2m}; when φ_{2m} goes to zero, the effective interaction parameter χ_{13}^{e} is equal to the usual binary value χ_{13} whereas in the limit that φ_{2m} approaches unity (thereby meaning that component 1 is necessarily interacting only with species 2), the effective interaction parameter χ_{13}^{e} approaches the value of χ_{12}. The same interpretation holds for χ_{13}^{e} as φ_{1m} varies between its own bounds. The form of eqs 10 and 11 are similar to the one proposed by Mulder et al.[23] The distinction between Mulder et al.'s definition and the form proposed here is that the former was defined by two unknown adjustable coefficients (a_{13} and b_{13}). As shown below, this renormalization scheme has reasonable predictive capabilities. To the authors' knowledge, the concept of rescaling the interaction parameters in this simple way for multicomponent swelling of networks does not appear elsewhere in the literature.

Substituting the definition of the solute−polymer interaction parameters given by eqs 10 and 11 in eq 2 to account for the renormalization of the interaction parameters and differentiating the resulting free energy expression with respect to the component mole number provides expressions for the chemical potentials of the two solute species. The chemical potentials for components 1 and 2 become

$$\Delta\mu_{1m} = RT\left[\ln\varphi_1 + 1 - \varphi_1 - \frac{V_1}{V_2}\varphi_2 + (\chi_{12}\varphi_2 + (a_{13} + b_{13}\varphi_2)\varphi_3)(1 - \varphi_1) - \varphi_1\varphi_2\varphi_3 b_{13} - \frac{V_1}{V_2}(a_{23} + b_{23}\varphi_1)\varphi_2\varphi_3 + \frac{V_1}{V_2}\varphi_2\varphi_3(\varphi_2 + \varphi_3)b_{23} + \rho_e V_1\left(\varphi_3^{1/3} - \frac{1}{2}\varphi_3\right)\right] \tag{12}$$

$$\Delta\mu_{2m} = RT\left[\ln\varphi_2 + 1 - \varphi_2 - \frac{V_2}{V_1}\varphi_1 + \left(\frac{V_2}{V_1}\chi_{12}\varphi_1 + (a_{23} + b_{23}\varphi_1)\varphi_3\right)(1 - \varphi_2) - \varphi_1\varphi_2\varphi_3 b_{23} - \frac{V_2}{V_1}(a_{13} + b_{13}\varphi_2)\varphi_1\varphi_3 + \frac{V_2}{V_1}\varphi_1\varphi_3(\varphi_1 + \varphi_3)b_{13} + \rho_e V_2\left(\varphi_3^{1/3} - \frac{1}{2}\varphi_3\right)\right] \tag{13}$$

Equations 12 and 13 can be used in place of eqs 4 and 5 when solving the phase equilibrium problem governed by eqs 8 and 9.

The solution procedure for simultaneously solving eqs 8 and 9 is shown in the block diagram of Figure 1. The parameters of the model include the two molar volumes, the various interaction parameters, and the cross-link density (V_1, V_2, χ_{12}, χ_{13}, χ_{23}, ρ_e). The value of φ_{1s} is fixed, and initial trial values for φ_{1m} and φ_{2m} are assumed. Equation 8 is then solved to find φ_{1m}, and using this new value eq 9 is solved for φ_{2m}. These calculated values are compared against the trial values for convergence; if they have changed since the prior iteration, they are adopted as the new trial values and the procedure is repeated. Once both concentrations within the membrane are converged, the concentration of the solvent, φ_{1s}, is incremented, and the whole procedure is repeated so that the membrane concentrations can be calculated as a function of the solvent concentration.

Materials and Methods

NBR (DN003 a poly(acrylonitrile-*co*-butadiene) random copolymer having 50 mol % acrylonitrile, a Mooney viscosity = 70−85, and ρ = 1.02 g/cm^3) was obtained from Zeon Chemicals. The trifunctional acrylic ester coagent SR517 was obtained from

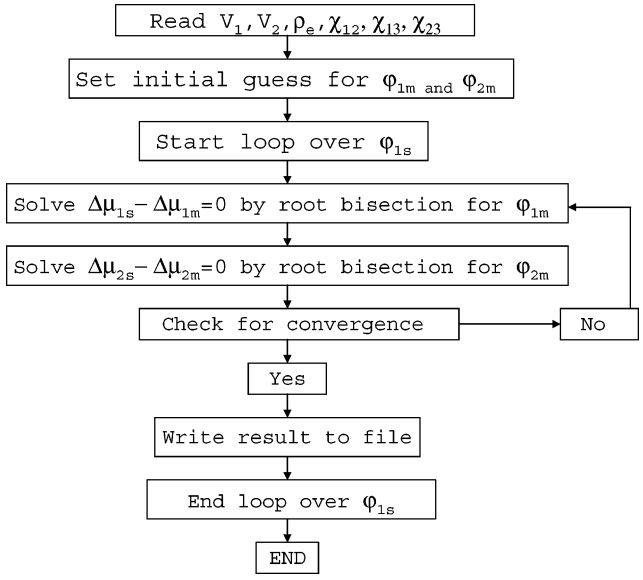

Figure 1. Numerical solution flow diagram.

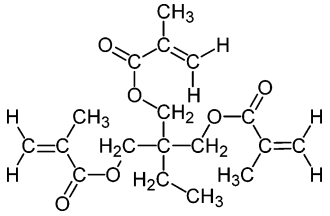

Figure 2. Chemical structure of trifunctional acrylic ester (2-ethyl-2-hydroxymethyl-1,3-propanediol trimethacrylate) determined from NMR spectral analysis.

Sartomer Co. The chemical structure of the trifunctional acrylic ester determined from NMR spectroscopy is given in Figure 2. Dicumyl peroxide, benzene, cyclohexane, and cyclohexanone were analytical grade chemicals obtained from Aldrich-Sigma.

To form cross-linked networks, a 12 wt % solution of un-cross-linked NBR in cyclohexanone was prepared, and a fixed amount of co-agent was added followed by a known amount of dicumyl peroxide. The resulting solution was well mixed. Nine stock solutions of the NBR were prepared with different amounts of coagent and peroxide in order to obtain films with different degrees of cross-linking. The samples were prepared by solution-casting onto float glass plates surrounded by masking tape and formed under controlled solute evaporation conditions by covering with aluminum pans. This minimized variation in film thickness, and importantly, eliminates preferential loss of curing agents in regions of high evaporation. The formed films were then thermally treated at 162 °C for 30 min in a vacuum oven.

An ARES 605 (TA Instruments) having a thin film fixture was used to determine the storage modulus of the membrane. The dimensions of the samples used were 5 mm wide and 60 mm long with typical thicknesses of several hundred microns. To avoid rough edges on the sides of the samples, a single stroke with a sharp razor blade was applied when cutting samples. A micrometer caliper was used to measure exact sample thickness. The film to be tested was mounted onto the thin film fixture and allowed to equilibrate to the testing temperature for ~30 min before beginning the test; a slight pretension was applied to the sample. Dynamic frequency sweeps ($10^{-2}-10^{2}$ Hz) were performed at constant temperatures between 30 and 195 °C. The temperature and frequency ranges chosen resulted in well-defined curves, showing a storage modulus plateau at low frequencies. Prior to performing the dynamic frequency sweeps, dynamic strain sweeps were conducted in order to determine appropriate strains to ensure that all measurements were within the linear viscoelastic region. Time−temperature superposition of the data obtained was performed to create a master curve shifted to a reference temperature of 60 °C. The storage modulus obtained from the plateau region of the master curve was used to determine the cross-linking density by applying the theory of rubber elasticity (i.e., $\rho_e = E/3RT$). To obtain the value of the modulus in the plateau region, experimental data were fit to a series of exponential function of the form shown in eq 14, and the function evaluated at $\omega = 0$ is taken to be the approximated modulus value.

$$E' = A_1 \exp(-\omega/t_1) + A_2 \exp(-\omega/t_2) + A_3 \exp(-\omega/t_3) + y_0 \quad (14)$$

In eq 14, ω denotes the frequency; the terms A_i, t_i ($i = 1, 2, 3$), and y_0 are constants and have values that depend on the specific system being evaluated.

DSC experiments were performed on the dry membrane samples, using ~20 mg of mass, sealed in aluminum pans. A Perkin-Elmer DSC 7 instrument was used. Samples were conditioned by heating from −80 to 140 °C at 20 °C/min; samples were then held at 140 °C for 5 min and subsequently cooled to −80 °C and held at this temperature for 5 min. Thermograms were recorded on the second heating from −80 to 140 °C at 20 °C/min. The T_g for each of the blends was determined using the half-C_p method for calculating T_g. This method estimates the T_g by reporting the point on the heat flow curve where the specific heat change is half of the change in the completed transition. In all cases, only a single T_g was observed, implying a homogeneous morphology.

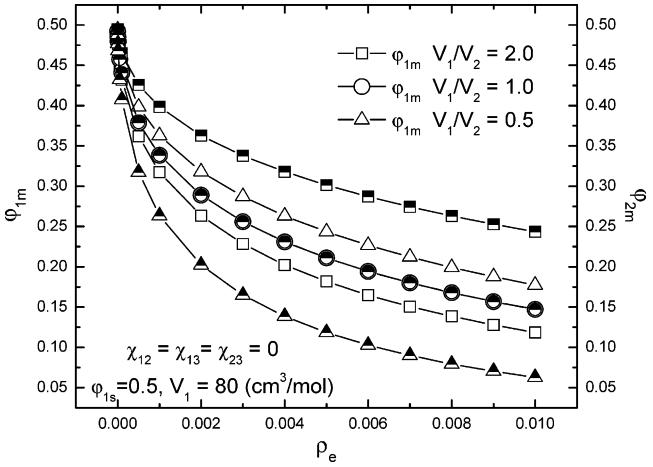

Figure 3. Effects of cross-link density and molecular volumes on solute solubilities in an athermal system. Open symbols refer to component 1 (φ_{1m}) and shaded symbols to component 2 (φ_{2m}).

Dry films having a dimension of 30 mm in length and breadth were cut from nine membrane samples each having different coagent and peroxide concentrations. Film thickness was measured using a micrometer caliper. Films were weighed before they were immersed in a closed bottle containing benzene, cyclohexane, or a mixture of both. The density of the dried films was averaged over the number of films taken from the "parent" sample. Films were removed from the bottle at certain time intervals and blotted dry with a Kimwipe. The films were weighed until no change in weight was observed over several hours of immersion time.

Flory−Huggins interaction parameters were determined from the pure component equilibrium swelling of the membrane films. The degree of swelling, DS, was determined using eq 15

$$\mathrm{DS} = \left(\frac{W_f - W_i}{W_i}\right)100 \quad (15)$$

where W_f is the final weight of swollen polymer film at equilibrium and W_i is the initial weight of polymer film before exposure to the solvent mixtures.

Results and Discussion

Theory. In this section, various case studies are discussed to elucidate the physical effects present in the model. This is followed by a direct comparison with experimental data.

For constant interaction parameters Figure 3 shows that, as expected, increasing the cross-linking density leads to a decrease in solubility for both components. In addition, the ratio of molar volumes has been changed while keeping the molar volume of species 1 fixed at 80 cm^3/mol (roughly the size of benzene); it is clear that the model always predicts a greater solubility for the species with the smaller molar volume.

Figures 4 and 5 demonstrate the effect of changing χ_{12} in an otherwise athermal system ($\chi_{13} = \chi_{23} = 0$); Figure 4 corresponds to the case of constant χ's, and Figure 5 corresponds to the case of renormalized χ's according to eqs 10 and 11. In both figures, the molar volumes for the solutes are assumed to be equal ($V_1 = V_2 = 80$ cm^3/mol), and the cross-link density is set to a value typical of the experimental results described below ($\rho_e = 0.003$ mol/cm^3).

Considering the constant interaction parameter case of Figure 4. When the system is completely athermal ($\chi_{12} = 0$, triangles in the figure), the expected linear relationship between concentration in the network and concentration in the contacting solution is observed. That is, in this *singular case* the equilibrium

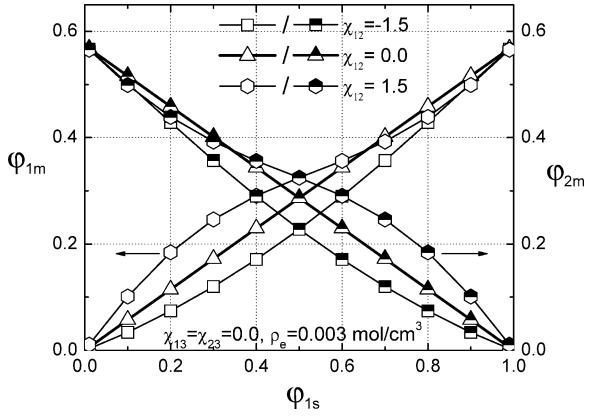

Figure 4. Effect of χ_{12} in an otherwise athermal system ($\chi_{13} = \chi_{23} = 0$) on the volume fractions of components 1 and 2 in the swollen polymer without renormalization of χ_{13} and χ_{23}. Open symbols refer to component 1 (φ_{1m}) and shaded symbols to component 2 (φ_{2m}).

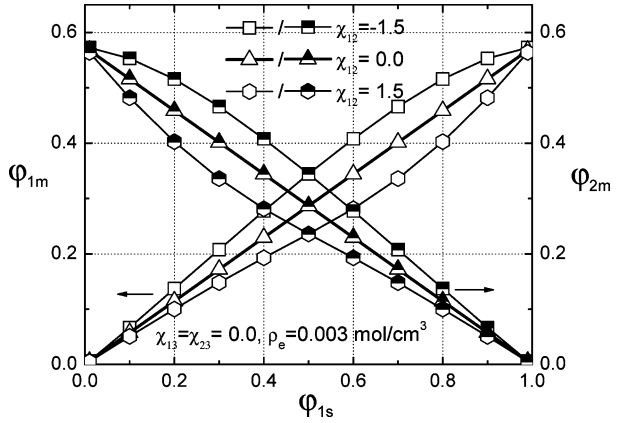

Figure 5. Effect of χ_{12} with renormalization in an otherwise athermal system ($\chi_{13} = \chi_{23} = 0$) on the volume fractions of components 1 and 2 in the polymer network. Open symbols refer to component 1 (φ_{1m}) and shaded symbols to component 2 (φ_{2m}).

may be described in terms of a simple partition coefficient, $K = \varphi_{1m}/\varphi_{1s}$. In any case for which either molar volumes are unequal or interactions exists, such a constant partition coefficient model is erroneous.

Figure 4 also shows the cases where the two solutes have very favorable interactions ($\chi_{12} = -1.5$) and very unfavorable interactions ($\chi_{12} = 1.5$). Effects associated with changing this interaction are immediately evident by examining the results for a 50:50 mixture ($\varphi_{1s} = 0.5$). As the solute−solute interaction parameter becomes more favorable, the solubility of both solutes in the network decreases. In the case of favorable solute−solute interactions ($\chi_{12} = -1.5$), the concentrations of both species are always lower than in the athermal case independent of the concentration of the mixed solvent. This is intuitively understood—favorable solvent−solvent interaction provides a driving force for retention of solutes in the solvent phase. However, in the case of unfavorable interactions, an interesting transition occurs at feed compositions of approximately 30 and 70 vol % ($\varphi_{1s} = 0.3$, $\varphi_{1s} = 0.7$); the dilute species is excluded from the solvent phase and pushed into the network phase while the concentrated species is retained. This can be understood by recognizing that for the dilute species the interaction in the solvent phase (where $\chi_{12} = 1.5$) is unfavorable compared to its interaction with the network phase (where $\chi_{13} = 0.0$). These energetic interactions favoring solubility in the membrane phase are balanced against unfavorable chain stretching entropic effects so that not all of the dilute species is pushed into the network. Interestingly,

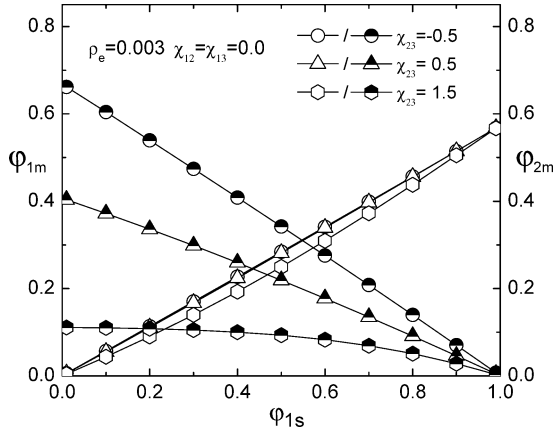

Figure 6. Effects of χ_{23} on the volume fractions of components 1 and 2 ($\chi_{12} = \chi_{13} = 0$) dissolved in the network without interaction parameter renormalization. Open symbols refer to component 1 (φ_{1m}) and shaded symbols to component 2 (φ_{2m}).

because moving one of the dilute species molecules into the network eliminates unfavorable solute−solute interactions in the solvent phase, the net effect is to have a *decreased solubility at high concentrations* relative to the athermal case for *unfavorable solute−solute interactions*. This counter-intuitive result is easily understood within the context of the present model and demonstrates the importance of understanding solute−solute coupling effects when designing elastomeric networks for a wide range of applications.

When the interaction parameters undergo renormalization, the results are significantly affected as illustrated in Figure 5. Again in the athermal case, the simple linear relationship between concentration in the contacting mixture and concentration in the network is observed. Effects associated with the renormalization are immediately evident by again examining the results for a 50:50 mixture ($\varphi_{1s} = 0.5$). In this case, the rankings of the solubility are reversed relative to the constant interaction parameter case. For favorable solute−solute interactions ($\chi_{12} = -1.5$), the concentrations of both solutes are now *higher* than in the athermal case, and this is independent of the concentration of the mixed solvent. This seemingly counter-intuitive result comes from the fact that the membrane phase becomes energetically more favorable as the solutes dissolve into it; that is, the effective membrane solute interaction parameters are no longer zero but are in fact negative. In the case of unfavorable solute−solute interactions the solutes are now less soluble. These phenomena can be understood by examining eqs 10 and 11; the solute−membrane interaction parameter is renormalized to include a contribution from χ_{12} thus altering the effective energetics.

In all cases exhibited in Figures 4 and 5, it is observed that the volume fraction of a given component in the network increases monotonically as the volume fraction of the corresponding component increases in the mixed solvent contacting the network. Interestingly, this is not always necessarily true as demonstrated next.

In Figures 6 and 7 the effects of changing the interaction of solute-2 with the network-3 (χ_{23}) is explored for the case of constant and renormalized interactions, respectively. Examining the constant interaction parameter case of Figure 6, the results show the expected trend—as χ_{23} is made more favorable, greater amounts of solute-2 are dissolved in the network. Interestingly, as the interaction is made highly unfavorable, a near plateau in solute-2 solubility is observed; that is, the solubility of component 2 becomes nearly *independent* of its concentration

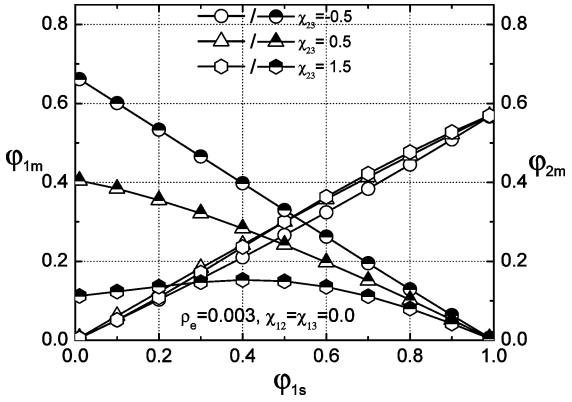

Figure 7. Effects of χ_{23} on the volume fractions of components 1 and 2 dissolved in the network with renormalization. Open symbols refer to component 1 (φ_{1m}) and shaded symbols to component 2 (φ_{2m}).

in the contacting mixed solvent. It is again worth emphasizing that the solubility in the network cannot be related to the concentration in the contacting phase through a simple partition coefficient in anything except the athermal case. Turning attention to the effects of changing χ_{23} on the solubility of component 1, very subtle effects are present. Because the athermal interaction of solute-1 with solute-2 in the mixed solvent phase is equal to the interaction of solute-1 with network-3 phase ($\chi_{13} = \chi_{12}$), the observed changes in solubility in the network are not directly enthalpic in their origin and so must be due to entropic effects. These entropic effects give rise to surprising and fascinating behavior; the solubility of solute-1 is *suppressed relative to the athermal case* for unfavorable ($\chi_{23} \geq 1.5$) solute-2 with network-3 interactions. In this case of unfavorable solute-2 interactions, species 2 is energetically excluded from the network. In contrast, species 1 has the same energetic environment in the solvent and network ($\chi_{13} = \chi_{12}$); however, the entropy of mixing is maximized in the solvent phase. That is, the lack of another low molecular weight species in the network phase to mix with means that from an entropic perspective the solvent phase is preferred. This interpretation is supported by noting that the maximum suppression of species 1 in the network phase (greatest deviation from the athermal case) takes place at the $\varphi_{1s} = 0.5$ solvent concentration; this is the point where the entropy of mixing in the solvent phase is maximized.

The effects of renormalizing the interaction parameters in the case of changing χ_{23} are shown in Figure 7. Qualitatively, the behavior is very similar to the case of constant χ parameters except for the different trend observed for the effect of χ_{23} on the volume fraction of component 1 in the membrane. In the case of constant interaction parameters, φ_{1m} increases slightly as χ_{23} changes from 1.5 to -0.5; a different observation occurs for the renormalized χ where the reverse trend is observed. That is, φ_{1m} increases as χ_{23} changes from -0.5 to 1.5, with a marked difference in φ_{1m} values. This observation could be ascribed to the fact that at $\chi_{23} \geq 0.5$ the interaction of component 1 with the membrane ($\chi_{13} = 0.0$) is interpreted as a favorable interaction over that of component 2. Notably, the concentration of species 2 in the membrane ($\chi_{23} = 1.5$) does actually pass through a slight maximum with increasing concentration. This counterintuitive behavior is a reflection of *cosolvency effects*—the presence of species 1 in the network phase helps solubilize component 2. Renormalization means that the effective interaction, χ_{23}^{e}, becomes less unfavorable than the original value of $\chi_{23} = 1.5$.

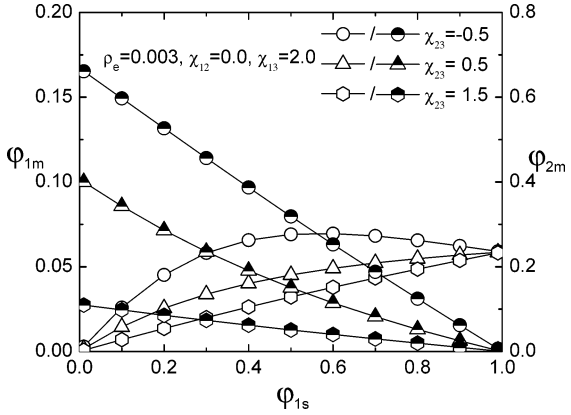

Figure 8. Effect of χ_{23} on the volume fractions of component 1 and 2 ($\chi_{12} = 0.0$, $\chi_{13} = 2.0$) in the swollen polymer, without renormalization of χ_{13} and χ_{23}. Open symbols refer to volume fractions of component 1 (φ_{1m}) and shaded symbols to component 2 (φ_{2m}).

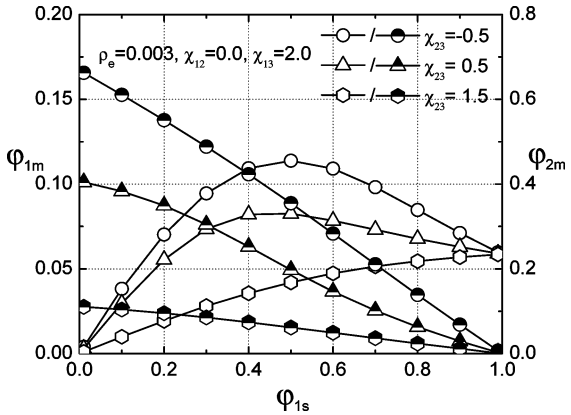

Figure 9. Effects of χ_{23} on the volume fractions of components 1 and 2 dissolved in the network with renormalization. Open symbols refer to volume fractions of component 1 (φ_{1m}) and shaded symbols to component 2 (φ_{2m}).

Figures 8 and 9 illustrate the effect of changing χ_{23} for the special case where solute-1 has a different energetic environment in the solvent and network ($\chi_{12} \neq \chi_{13}$); this is unlike the previous case discussed in which $\chi_{12} = \chi_{13} = 0$. Figure 8 corresponds to the case of constant χ's, and Figure 9 corresponds to the case of renormalized χ's. The highly unfavorable interaction between component 1 and the network ($\chi_{13} = 2.0$) suggests that component 1 is likely to be excluded from the polymer network. The trends observed (Figures 8 and 9) for the effect of changing χ_{23} on φ_{2m} as a function of φ_{1s} is similar to that in Figures 6 and 7, except for the fact that the concentration of species 2 does not pass through a maximum at ($\chi_{23} = 1.5$). However, a significant difference is observed in the nature of the trends of φ_{1m} as a function of φ_{1s} at different values of χ_{23}; the concentration of component 1 passes through a very apparent maximum at $\chi_{23} = -0.5$. A significant increase in the volume fraction of solute-1, for a given feed concentration, is observed as the interaction parameter between component 2 and the polymer network is varied. This is dissimilar from the behavior in Figures 6 and 7 in which only a slight increase in φ_{1m} is observed. The enhancement of the composition of solute-1 in the membrane for $\chi_{23} = -0.5$ suggests that the presence of a strong solute-2/network-3 interaction changes the network environment to one that increases the solubility of component 1.

The renormalized χ's case in Figure 9 exhibits similar trends for the plots of φ_{1m} and φ_{2m} as a function of φ_{1s} when compared to Figure 8. However, the effects are more pronounced for

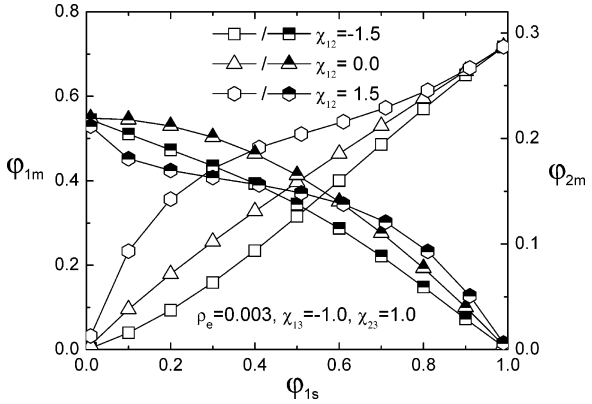

Figure 10. Effect of χ_{12} on the volume fractions of components 1 and 2 in the swollen polymer, without renormalization of χ_{13} and χ_{23}. Open symbols refer to volume fractions of component 1 (φ_{1m}) and shaded symbols to component 2 (φ_{2m}).

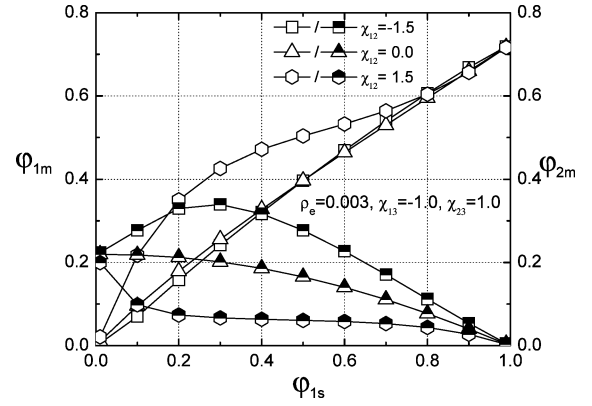

Figure 11. Effect of χ_{12} with renormalization ($\chi_{13} = -1.0$ and $\chi_{23} = 1.0$) on the volume fractions of components 1 and 2 in the polymer network. Open symbols refer to volume fractions of component 1 (φ_{1m}) and shaded symbols to component 2 (φ_{2m}).

results compared at the same set of interaction parameter values. Again, it is observed that the renormalization scheme enhances the cosolubility effects.

In Figures 10 and 11, the effects of changing χ_{12} on a system in which χ_{13} is less than χ_{23} ($\chi_{13} = -1.0$ and $\chi_{23} = 1.0$) are presented. Figure 10 corresponds to the case of constant χ's, and Figure 11 corresponds to the case of renormalized χ's. The negative value of χ_{13} favors more of solute-1 disolving into the polymer network than solute-2; unfavorable solute−solute interactions further enhance this effect. That is, Figure 10 shows that, for a given feed concentration, the volume fraction of component 1 in the network increases as the interaction between component 1 and 2 becomes less favorable.

Figure 11 shows the corresponding renormalized case to Figure 10. It is observed for that the effect of changing χ_{12} on the solubility of solute-2 is now monotonic. Again, the inclusion of a χ_{12} contribution to the solute−network interactions changes the qualitative behavior. For example, favorable solute−solute interactioins ($\chi_{12} = -1.5$) lead to greater solubility of solute-2 in the membrane. Such coupling effects cause the concentration of component 2 in the network to exhibit a maximum and a minimum when $\chi_{12} = -1.5$ and 1.5, respectively.

In summary, the two versions of the multicomponent swelling model described by eqs 4−13 show a wide variety of interesting and sometimes counter-intuitive behaviors. Careful examination of the results does lead to the conclusion that solute−solute coupling effects in multicomponent swelling are of utmost importance in a variety of cases.

Table 2. Glass Transition Temperature (T_g), Density (ρ), and Elastic Modulus (E') of Membranes As Determined Experimentally

sample ID	T_g (°C)	ρ (g/cm^3)	E' (MPa)
NA1	-5.6 ± 0.15	1.022 ± 0.076	3.26 ± 0.90
NA3	-5.0 ± 0.15	0.990 ± 0.075	8.46 ± 1.05
NA5	-3.7 ± 0.15	1.034 ± 0.078	16.0 ± 2.7
NB1	-5.1 ± 0.15	0.999 ± 0.074	6.13 ± 0.58
NB3	-5.0 ± 0.15	1.022 ± 0.075	10.3 ± 1.2
NB5	-3.6 ± 0.15	1.035 ± 0.076	17.9 ± 2.5
NC1	-5.7 ± 0.15	0.986 ± 0.073	15.9 ± 2.2
NC3	-4.5 ± 0.15	1.039 ± 0.080	19.4 ± 4.5
NC5	-1.6 ± 0.15	1.021 ± 0.076	29.9 ± 2.3

Experiments

Sample descriptions and formulations are given in Table 1 along with the swelling data and derived interaction parameters. Results for the glass transition temperature (T_g), density (ρ), and modulus (E') measurements are shown in Table 2. The amount of peroxide added to the system increases the degree of cross-linking, as shown by the increases in both T_g and modulus E'. The cross-linking is also significantly increased by the amount of coagent added to the sample. The double bonds in the coagent (2-ethyl-2-hydroxymethyl-1,3 propanediol trimethacrylate) structure are opened up creating additional cross-linking sites.

The samples prepared span an order of magnitude in their low-frequency moduli. An example master curve for a sample cross-linked using 10 wt % coagent and 3 wt % dicumyl peroxide is shown in Figure 13. Moduli increase with increasing coagent concentration.

Degree of swelling (DS) data were taken as a function of benzene−cyclohexane composition (measured as weight fraction of benzene, w_{BZ}). Results are denoted by the filled-square symbols in Figures 14−19. Samples exposed to pure cyclohexane show negligible swelling due to the high polarity of the 50% acrylonitrile by weight NBR employed in this work. However, an increase in the benzene composition from 0 to 25 % resulted in a dramatic increase in the swelling. The effect of coagent on swelling is more noticeable in the sample having high level of peroxide, for example 3 and 5%; this observation may be explained by the fact that at low level of peroxide content the coagent cannot be fully utilized.

Table 1. Solute−Membrane Interaction Parameters and Volume Fractions Determined from Swelling Data

sample ID	coagent content (wt %)	peroxide content (wt %)	$\chi_{BZ-membrane}$	$\chi_{CH-membrane}$	$\varphi_{membrane}$ (in BZ)	$\varphi_{membrane}$ (in CH)
NA1	0.1	1	0.528	2.836	0.365 ± 0.040	0.975 ± 0.150
NA3	0.1	3	0.236	2.507	0.340 ± 0.030	0.965 ± 0.150
NA5	0.1	5	0.137	2.745	0.407 ± 0.040	0.975 ± 0.150
NB1	1	1	0.385	2.818	0.355 ± 0.040	0.975 ± 0.140
NB3	1	3	0.227	2.731	0.366 ± 0.040	0.973 ± 0.140
NB5	1	5	−0.060	2.898	0.375 ± 0.040	0.979 ± 0.140
NC1	10	1	0.040	2.674	0.379 ± 0.040	0.973 ± 0.140
NC3	10	3	−0.054	2.463	0.389 ± 0.040	0.966 ± 0.150
NC5	10	5	−0.092	2.908	0.460 ± 0.050	0.981 ± 0.150

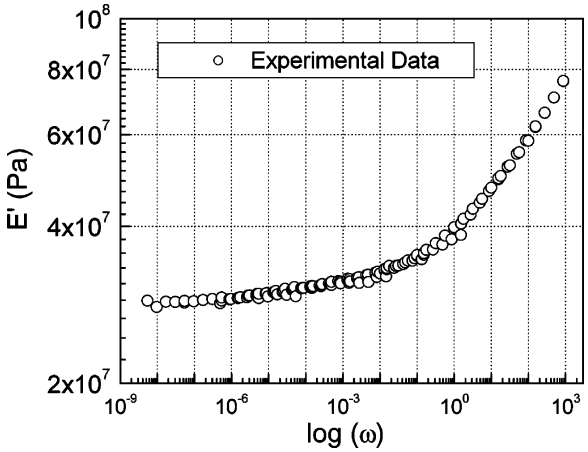

Figure 12. Master curve obtained from frequency−temperature superposition analysis for sample NC5.

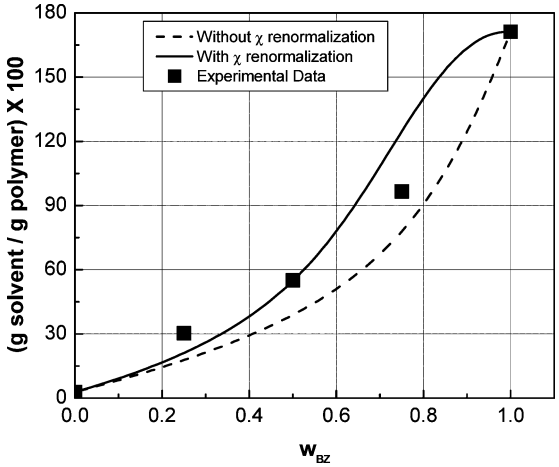

Figure 13. Effect of feed composition on the degree of swelling of membrane containing 0.1 and 3 wt % of coagent and peroxide, respectively.

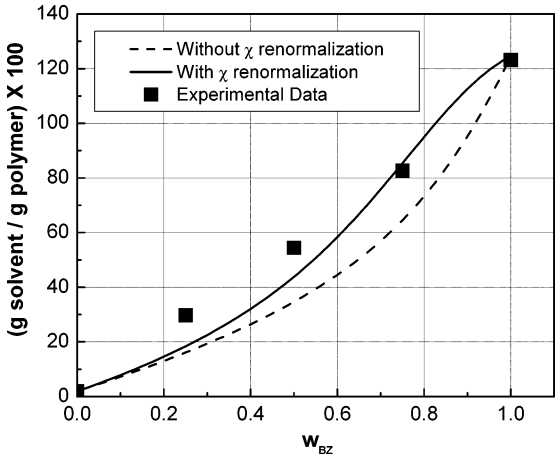

Figure 14. Effect of feed composition on the degree of swelling of membrane containing 0.1 and 5 wt % of coagent and peroxide, respectively.

Interaction parameters (see Table 1) determined from swelling in pure components show that the addition of more coagent to a sample results in a stronger affinity for benzene. On the other hand, a decrease in the benzene−network interaction parameter was observed when the cross-linking density increases by the addition of more peroxide, for samples having the same coagent amount. These results contrast with previous observations that increasing the cross-linking density increases the interaction

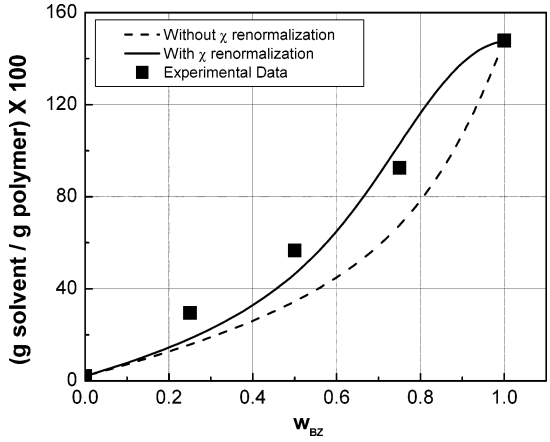

Figure 15. Effect of feed composition on the degree of swelling of membrane containing 1 and 3 wt % of coagent and peroxide, respectively.

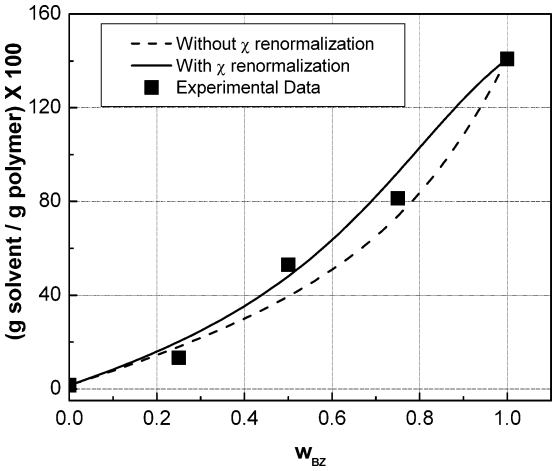

Figure 16. Effect of feed composition on the degree of swelling of membrane containing 1 and 5 wt % of coagent and peroxide, respectively.

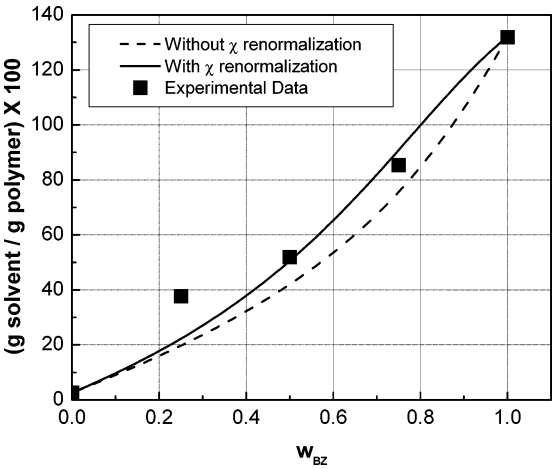

Figure 17. Effect of feed composition on the degree of swelling of membrane containing 10 and 3 wt % of coagent and peroxide, respectively.

parameter.[7] It is to be noted though that in the present case a coagent is included.

Comparisons of results predicted using the new models with experimental data are shown in Figures 14−19. The solid and dash lines are model predictions using the multicomponent Flory−Rehner equations with and without χ renormalization, respectively. In all cases a constant $\chi_{12} = 0.5$ was used as the

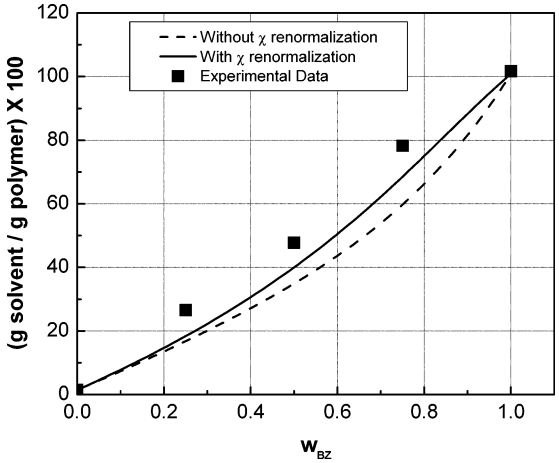

Figure 18. Effect of feed composition on the degree of swelling of membrane containing 10 and 5 wt % of coagent and peroxide, respectively.

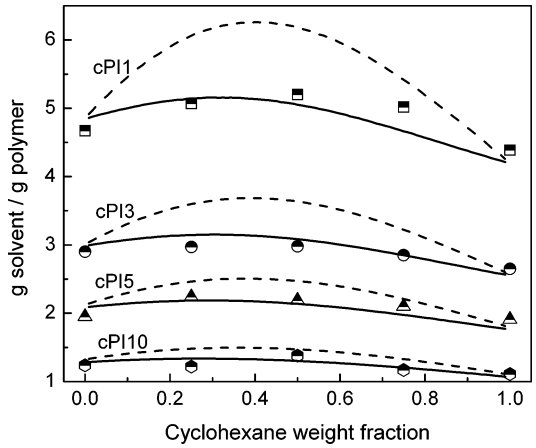

Figure 19. Comparison of model predictions and experimental data obtained from literature. Symbols represent experimental data[24] from the work of Schlick et al. Solid and dash lines are model predictions using Flory−Rehner equations with and without χ renormalization, respectively.

value of the cyclohexane−benzene interaction parameter.[24] Overall, results show that the introduction of the effective interaction parameter improves the quantitative description of the experimental data. Generally, the constant χ parameter model underprediicts the total swelling, an effect attributable to underpredicting the effects of solute−solute coupling.

The validity of the proposed renormalization was further tested using the data of Schlick and co-workers[24] for the swelling of polyisoprene networks, cross-linked to different degrees, in benzene−cyclohexane mixtures. Reported values[24] for the interaction parameters and the molar volume of solvents were adopted for use in the present models. As a result of the difference in the reported values for the cross-linking density determined from swelling in pure benzene vs pure cyclohexane, averages of the two values are used in the calculations. The results of this independent comparison are shown in Figure 19; the solid and dashed lines are again model predictions using Flory−Rehner equations with and without χ renormalization, respectively. It is observed that the model with χ renormalization shows a significant improvement in predictions than the constant interaction parameter model and exhibits a better prediction of the experimental data. This improved result is most noticeable in the result for sample cPI1; in this case the constant interaction parameter model result displays a significant deviation from experimental result and is not able to produce a quantitative description of the experimental data.

Conclusions

Two versions of a model for network swelling by binary solvent mixtures have been developed and tested against experimental data. Equations and numerical solution procedures for treating the full equilibrium problem of a binary mixed solvent in contact with a cross-linked polymeric network are presented. A novel renormalization provides a methodology for providing a set of compositionally dependent interaction parameters without the need for simply fitting data. Comparison of model results with swelling data for NBR in benzene−cyclohexane mixtures shows that the renormalization approach provides better predictive capability that the constant interaction parameter methodology. This is true both for data generated in our own laboratory as well as for independent data appearing in the literature.

Calculated case studies for different values of the cross-link density and interaction parameters show novel phenomena in certain cases including *decreasing* concentration in the membrane with *increasing* component concentration in the contacting mixture. Several explainable but counter-intuitive findings point out the necessity of having a quantitative description of multicomponent swelling when designing elastomeric networks for a wide variety of applications ranging from membranes for chemical separations to biochemical protective clothing to hydrogels for the controlled release of drugs and other agents.

References and Notes

(1) Park, H.-C.; Meertens, R. M.; Mulder, M. H. V. *Ind. Eng. Chem. Res.* **1998**, *37*, 4408−4417.
(2) Wang, H.; Ugomori, T.; Wang, Y.; Tanaka, K.; Kita, H.; Okamoto, K.-I.; Suma, Y. *J. Polym. Sci., Part B: Phys.* **2000**, *38*, 1800−1811.
(3) Meuleman, E. E. B.; Bosch, B.; Mulder, M. H. V.; Strathmann, H. *AIChE J.* **1999**, *45*, 2153−2160.
(4) Zhang, S. *Nat. Mater.* **2004**, *3*, 7−8.
(5) Kim, J. J.; Park, K. *Bioseparation* **1999**, *7*, 177−184.
(6) Wang, K. L.; Burban, J. H.; Cussler, E. L. *Adv. Polym. Sci.* **1993**, *110*, 67−79.
(7) McKenna, G. B.; Flynn, K. M.; Chen, Y. *Polymer* **1990**, *31*, 1937−1945.
(8) Flory, P. J.; Rehner, J. *J. Chem. Phys.* **1943**, *11*, 521−526.
(9) Mulder, M. H. V.; Smolders, C. A. *J. Membr. Sci.* **1984**, *17*, 289−307.
(10) Yoo, J. S.; Kim, S. J.; Choi, J. S. *J. Chem. Eng. Data* **1999**, *44*, 16−22.
(11) McKenna, G. B.; Crissman, J. M. *J. Polym. Sci., Part B: Polym. Phys.* **1997**, *35*, 817−826.
(12) McKenna, G. B.; Horkay, F. *Polymer* **1994**, *35*, 5737−5742.
(13) Gottlieb, M.; Gaylord, R. J. *Macromolecules* **1984**, *17*, 2024−2030.
(14) Gusler, G. M.; Cohen, Y. *Ind. Eng. Chem. Res.* **1994**, *33*, 2345−2357.
(15) Hild, G. *Polymer* **1997**, *38*, 3279−3293.
(16) Brannon-Peppas, L.; Peppas, N. *Chem. Eng. Sci.* **1991**, *46*, 715−722.
(17) Hooper, H. H.; Baker, J. P.; Blanch, H. W.; Prausnitz, J. M. *Macromolecules* **1990**, *23*, 1096−1104.
(18) Neuburger, N. A.; Eichinger, B. E. *Macromolecules* **1988**, *21*, 3060−3070.
(19) Krigbaum, W. R.; Carpenter, D. K. *J. Polym. Sci.* **1954**, *14*, 241−259.
(20) Bristow, G. M. *Trans. Faraday Soc.* **1959**, *55*, 1246.
(21) Masa, Z.; Pouchly, J.; Pribilova, J.; Biros, J. *J. Polym. Sci.: Symp.* **1975**, *53*, 271−282.
(22) Kargupta, K.; Datta, S.; Sanyal, S. K. *J. Membr. Sci.* **1997**, *124*, 253−262.
(23) Mulder, M. H. V.; Franken, T.; Smolders, C. A. *J. Membr. Sci.* **1985**, *22*, 155−173.
(24) Schlick, S.; Gao, Z.; Matsukawa, S.; Ando, I.; Fead, E.; Rossi, G. *Macromolecules* **1998**, *31*, 8124−8133.
(25) Iwatsubo, T.; Ogasawara, K.; Yamasaki, A.; Masuoka, T.; Mizoguchi, K. *Macromolecules* **1995**, *28*, 6579−6585.
(26) Iwatsubo, T.; Masuoka, T.; Mizoguchi, K. *J. Polym. Sci., Part B: Polym. Phys.* **1994**, *32*, 7−13.
(27) Jonquieres, A.; Perrin, L.; Durand, A.; Arnold, S.; Lochon, P. *J. Membr. Sci.* **1998**, *147*, 59−71.

(28) Koningsveld, R.; Kleintjens, L. A. *Macromolecules* **1971**, *4*, 637−641.
(29) Nandi, S.; Winter, H. H. *Macromolecules* **2005**, *38*, 4447−4455.
(30) Tereshatov, V. V.; Senichev, V. Y.; Denisyuk, E. Y. Equilibrium swelling in binary solvents. In *Handbook of Solvents*; Wypych, G., Ed.; Chemtec Publishing: Toronto, 2001; p 325.
(31) Flory, P. J. *Principles of Polymer Chemistry*; Cornell University Press: Ithaca, NY, 1953; p 549.
(32) Praustniz, J. M.; Lichtenthaler, R. N.; Azevedo, E. G. d. *Molecular Thermodynamics of Fluid-Phase Equilibria*, 3rd ed.; Prentice Hall: Englewoods Cliffs, NJ, 1998; p 290.

MA0618124